

# Energy loss in a strongly coupled anisotropic plasma

Kazem Bitaghsir Fadafan<sup>a1</sup>, Hesam Soltanpanahi<sup>b2</sup>

<sup>a</sup>*Physics Department, Shahrood University of Technology, Shahrood, Iran*

<sup>b</sup>*National Institute for Theoretical Physics, Gauteng  
School of Physics and Center for Theoretical Physics,  
University of the Witwatersrand,  
WITS 2050, Johannesburg, South Africa*

## Abstract

We study the energy loss of a rotating infinitely massive quark moving, at constant velocity, through an anisotropic strongly- coupled  $\mathcal{N} = 4$  plasma from holography. It is shown that, similar to the isotropic plasma, the energy loss of the rotating quark is due to either the drag force or radiation with a continuous crossover from drag-dominated regime to the radiation dominated regime. We find that the anisotropy has a significant effect on the energy loss of the heavy quark, specially in the crossover regime. We argue that the energy loss due to radiation in anisotropic media is less than the isotropic case. Interestingly this is similar to analogous calculations for the energy loss in weakly coupled anisotropic plasma.

---

<sup>1</sup>e-mail:bitaghsir@shahroodut.ac.ir

<sup>2</sup>e-mail:hesam.soltanpanahisarabi@wits.ac.za

# Contents

<b>1</b>	<b>Introduction</b>	<b>1</b>
<b>2</b>	<b>The gravity background</b>	<b>3</b>
<b>3</b>	<b>Rotating string in a general background</b>	<b>4</b>
<b>4</b>	<b>Rotating string in strongly-coupled anisotropic plasma</b>	<b>7</b>
4.1	The energy loss . . . . .	10
<b>5</b>	<b>Analytic limits</b>	<b>14</b>
5.1	Ultra-relativistic limit . . . . .	15
5.2	Small $a/T$ limit . . . . .	17
<b>6</b>	<b>Comparison with the linear drag and the synchrotron radiation</b>	<b>18</b>
<b>7</b>	<b>Summary and discussion</b>	<b>20</b>
<b>A</b>	<b>Rotation in anisotropic plane</b>	<b>21</b>
<b>B</b>	<b>Linear drag in a general background</b>	<b>22</b>

## 1 Introduction

The experiments at Relativistic Heavy Ion Collisions (RHIC) and at the Large Hadron Collider (LHC) have produced a strongly-coupled quark–gluon plasma (QGP)(see review [1]). At a qualitative level, the data indicate that the QGP produced at the LHC is comparably strongly-coupled [2]. The QGP created at the LHC is expected to be closer to conformality than the case at RHIC [1]. The plasma created right after a heavy ion collision is anisotropic for a period of time,  $\tau < \tau_{\text{iso}}$  and becomes locally isotropic afterwards [3, 4, 5]. There are no known quantitative methods to study strong coupling phenomena in QCD which are not visible in perturbation theory (except by lattice simulations). A new method for studying different aspects of the QGP is the *AdS/CFT* correspondence [1, 6, 7, 8, 9].

The energy loss of partons is a useful probe of the QGP. One should notice that this quantity is not a direct experimental observable but it is related to the jet quenching parameter  $\hat{q}$ . This parameter is a signature of the QGP and initially was calculated from AdS/CFT correspondence in [10]. Although the energy loss can be due to various different mechanisms, two primary sources of the energy loss are collisions and radiation. The former is due to the scattering of the energetic partons with thermal quarks and gluons in the QGP, while the later is related to the Bremsstrahlung radiation during the interactions with the medium. Theoretical study of these phenomena needs strong-coupling tools and non-perturbative methods such as lattice QCD, which are inadequate to describe these time-dependent phenomena. A new method is to use the holographic principle and investigate the energy loss of heavy probes.

This method has yielded many important insights into the dynamics of strongly-coupled gauge theories. It has been used to investigate hydrodynamical transport quantities in various interesting strongly-coupled gauge theories where perturbation theory is not applicable.

Using this method, the energy loss due to collisions of heavy quarks was initially discussed in [11, 12]. They considered a heavy quark traveling with constant linear velocity through the plasma, and find the energy required to keep it in uniform motion. This energy is then given by the world-sheet momentum and falls across the horizon. On the other hand, the energy loss is proportional to the momentum of the heavy quark and one concludes that the energy loss mechanism can be considered as a drag force. Some extension of this calculation to more realistic models of QGP have been done in [13]. It should be noticed that the physically relevant setting is when there is no external force acting on the energetic parton. Then the moving probe is decelerating and here is the possibility of another important mechanism of energy loss, namely radiation [14, 15, 16]. Therefore, it is worthwhile to find interference between these two different mechanisms of the energy loss, the drag force and radiation.

By considering the quark rotating uniformly with constant velocity  $v$ , one can consider these two mechanisms of the energy loss at the same time.<sup>3</sup> The significant advantage offered by the analysis of this problem was explored in [17]. They determined the energy it takes to move a test quark along a circle of radius  $l$  with angular frequency  $\omega$  through the strongly-coupled plasma of  $\mathcal{N} = 4$  supersymmetric Yang-Mills (SYM) theory. The drag force and radiation for fixed  $v = l\omega$  are dominant when  $(\omega \rightarrow 0, l \rightarrow \infty)$  and  $(\omega \rightarrow \infty, l \rightarrow 0)$ , respectively. The extension of this calculation to the case of non-conformal plasma, which exhibits a confinement/deconfinement transition at a critical temperature, was done in [18]. They argued that in the low temperature limit the energy loss is completely due to glueball Bremsstrahlung. The motion of a heavy charged quark in a magnetic field was also analyzed in the vacuum of strongly-coupled conformal field theory in [19].

In this paper, we study the energy loss of a rotating quark in a strongly-coupled anisotropic plasma using the AdS/CFT correspondence. Anisotropy is very important during the initial phase after the QGP production in the heavy-ion collisions. It is related to this point that initially the system expands mainly along the collision axis. As a result, the plasma has significantly unequal pressures in the longitudinal and transverse directions. To model this medium, we consider an anisotropic  $\mathcal{N} = 4$  SYM plasma in which the  $x, y$  directions are rotationally symmetric, while the  $z$  direction corresponds to the beam direction [20]. The drag force and jet quenching parameter in this medium were calculated in [21, 22, 23]. It was found that the energy loss of partons depend on the relative orientation between the anisotropic direction and the velocity of the quark.

Another interesting feature of this anisotropic background is that the ratio of the shear viscosity to the entropy density violated KSS bound [25]. While the ratio in transverse direction saturates the KSS bound ( $\eta/s = 1/4\pi$ ), it was shown that the perturbation of the metric with an off-diagonal component (mixing the anisotropy direction with one of the isotropic directions) leads to a smaller ratio,  $\eta/s < 1/4\pi$  and it is a decreasing function of  $a/T$  [26, 27].<sup>4</sup> This is the first example of violation of KSS bound not involving higher derivative theories of gravity [28]. Also it was shown that the DC conductivity along (transverse) to the anisotropy direction is a decreasing (increasing) function of the ratio of the anisotropy parameter to the temperature [26].

---

<sup>3</sup> The interplay between the energy loss due to the radiation and the drag force can also be observed in the early times energy loss of a heavy quark [24]. This study has been done in the isotropic plasma, while one may expect that the results will be affected by considering the anisotropy in the real models.

<sup>4</sup>As in [20] we identify the temperature and the anisotropy parameter of the plasma by " $T$ " and " $a$ ", respectively.

Motivated by these considerations, in this paper we study the effect of anisotropy on the energy loss of heavy quark propagating through anisotropic medium. We consider the quark rotating uniformly with constant velocity in the  $xy$  plane. Two possible mechanisms of the energy loss are considered: drag force and radiation. We compare the energy loss in an anisotropic plasma to the isotropic case. For completeness, we will also compare the results with the drag force and jet quenching parameter found in an anisotropic plasma in the last section.

The article is organized as follows. In the next section, we introduce an anisotropic gravity solution which is a well-defined IIB supergravity dual to spatially anisotropic  $\mathcal{N} = 4$  SYM plasma at finite temperature. Then we will give a discussion about rotating string in a general background in section 3. For a background with  $SO(2)$  symmetry, we find the most general form of the equations of motion and the critical points of the rotating string in isotropic plane. This section will be very useful from technical point of view for our calculations. In section 4, we solve numerically the equations of motion of a rotating string in the anisotropic plasma (introduced in section 2) and find the energy loss of a heavy quark. Some analytic limits will be studied in section 5 and comparison with linear drag and radiation will be done in section 6. Finally, we will discuss our results and some possible extensions for future work in the section 7. To complete the investigation of sections 2 and 4, appendix A is devoted to discussion of a rotating quark in an anisotropic plane. In appendix B we give a brief general review of the drag force which is very useful for comparing our results in a special limit studied in section 5.

## 2 The gravity background

In this section we review the anisotropic background introduced in [20] which is the gravity dual to a deformation of  $\mathcal{N} = 4$  SYM adding a  $\theta$  term to the action. The geometry of this solution has two parts: a deformed  $AdS_5$ , which has spatially anisotropy but it is asymptotically  $AdS_5$ , and an  $S^5$  part. The deformation parameter,  $\theta$ , depends on the anisotropic spatial direction  $z$  as  $\theta = 2\pi n_{D7} z$ , where  $n_{D7}$  can be thought as the density of D7-branes homogeneously distributed along the anisotropic direction. The D7-branes wrap the  $S^5$  and two spacial directions of the  $AdS_5$  ( $xy$ -plane).

The type IIB supergravity solution in the string frame is given by [20]<sup>5</sup>

$$ds^2 = \frac{L^2}{u^2} \left( -\mathcal{F}\mathcal{B}dt^2 + dx^2 + dy^2 + \mathcal{H}dz^2 + \frac{du^2}{\mathcal{F}} \right) + L^2 e^{\phi/2} ds_{S^5}^2$$

$$\phi = \phi(u), \quad \chi = a z, \quad (2.1)$$

where  $\phi$ ,  $\chi$ , are the dilaton and axion fields respectively, and the anisotropy parameter is  $a = \frac{g_{\text{YM}}^2 n_{D7}}{4\pi}$ . The metric functions are  $\mathcal{F}$ ,  $\mathcal{B}$  and  $\mathcal{H}$  which depend on the holographic radial coordinate,  $u$ , the radius of horizon,  $u_H$ , and the anisotropy parameter,  $a$ . We choose the range  $0 < u < u_H$  for the holographic radial coordinate and the boundary is at  $u = 0$ .  $\mathcal{F}$  is the blackening function,  $\mathcal{F}(u_H) = 0$ , and the solution is asymptotically  $AdS_5$  where  $\mathcal{F}_b = \mathcal{B}_b = \mathcal{H}_b = 1$ . The solutions of the equations of motion are specified by two parameters, the horizon radius,  $u_H$ , and the value of dilaton at the horizon,  $\phi_h$ . From

---

<sup>5</sup>This is the finite-temperature generalization of the type IIB supergravity solution of [29], the drag force calculation in this case has been studied in [30].

the boundary theory point of view these parameters map to the temperature,  $T$ , and the anisotropy parameter,  $a$ . In Fig. 1, we show two solutions for different combinations of the parameters: Left  $\phi_h \simeq -0.22$  and  $u_H = 1$  (or  $T \simeq 0.33$  and  $a/T \simeq 4.4$ ), Right  $\phi_h \simeq -1.86$  and  $u_H = 1$  (or  $T \simeq 0.48$  and  $a/T \simeq 86$ ).

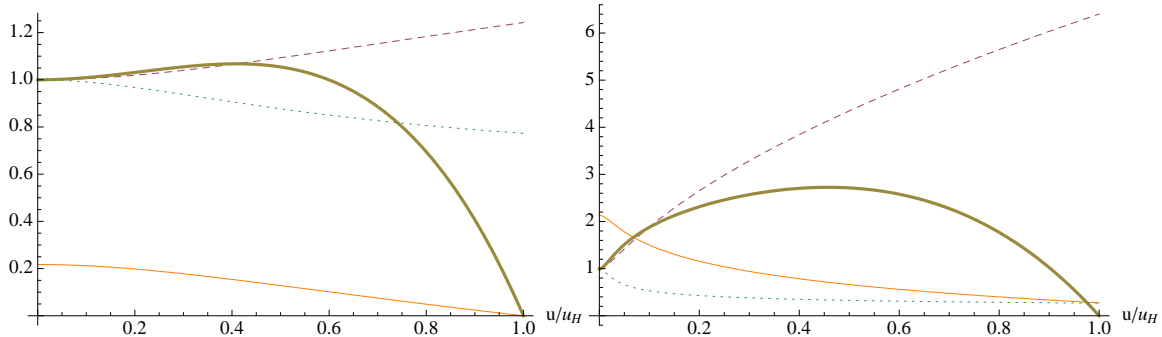


Figure 1: Metric functions  $\phi$  (orange),  $\mathcal{H}$  (dashed),  $\mathcal{F}$  (thick),  $\mathcal{B}$  (dotted) curves for two different parameters. Left:  $a/T \simeq 4.4$ , Right:  $a/T \simeq 86$ .

The metric functions are parameterized by two parameters, the dilaton field value at the horizon  $\phi_h$  and  $u_H$  or equivalently by  $T$  and  $a/T$ . At small  $a/T$ , the entropy density scales as in the isotropic case  $S_{iso} = \frac{\pi^2}{2} N_c^2 T^3$ , while at large  $a/T$  it scales as  $S_{aniso} = c_{ent} N_c^2 a^{1/3} T^{8/3}$ , where  $c_{ent}$  is a constant. To compare the results in the anisotropic plasma to that in the isotropic plasma, we consider two cases: the two plasmas can be taken to have the same temperatures but different entropy densities, or the same entropy densities but different temperatures. Each case leads to different results.

The field theory coordinates at the boundary are  $(t, x, y, z)$  and there is an  $SO(2)$  symmetry in the  $xy$  plane. We will consider our rotating test quark in this plane which can be interpreted as transverse plane to the beam. We find that, although the quark is moving in this plane, anisotropy has main effect on the transport properties. Appendix A is devoted to discussion of a rotating quark in an anisotropic plane.

One of the main feature of this anisotropic solution is the presence of a conformal anomaly [20] which leads to the fact that, the thermodynamics of the solution depend on the parameters  $T$  and  $a$  separately. This is the cause of broken diffeomorphism invariance in the holographic direction  $u$ . We will see that this is not the case for the rate of energy loss for a rotating string in this background which takes the form  $(dE/dt)_{aniso} = (dE/dt)_{iso} \hat{f}(a/T)$ . This kind of behavior is similar to the results of drag force and jet quenching parameter studied in [21, 22, 23].

In next section, we will find the equations of motion of a rotating string and we will discuss an approach to solve these equations as generally as possible. Then we will focus on the anisotropic solution (2.1) and by comparing the results with the isotropic  $AdS_5 \times S^5$  background, we investigate the effect of anisotropy on the energy loss of a rotating quark.

### 3 Rotating string in a general background

In this section, we will discuss technical details of studying rotating strings in a general background with  $SO(2)$  symmetry. We will use the results of this section during our calcu-

lations in the next sections. The general form of this static metric is given by

$$ds^2 = G_{tt}dt^2 + G_{\rho\rho}d\rho^2 + G_{\psi\psi}d\psi^2 + G_{zz}dz^2 + G_{uu}du^2, \quad (3.1)$$

In our coordinates,  $u$  denotes the holographic radial coordinate of the black hole geometry and  $t, \rho, \psi$  and  $z$  label the directions along the boundary at  $u = 0$ .

In the gravity dual, a heavy test quark corresponds to an open string with one endpoint on a D3-brane at  $u = 0$ . The string hangs down into the bulk, extending towards the black-hole horizon at  $u = u_H$ . In order to study the energy loss for a quark moving on a circle, we must first find the world-sheet of the string spiraling downward from the quark moving on a circle at  $u = 0$  and then calculate the energy flowing down the string. We choose to parameterize the two-dimensional world-sheet of the rotating string according to

$$X^\mu(\tau, \sigma) = (t = \tau, u = \sigma, \psi = \omega t + \theta(\sigma), \rho = \rho(\sigma), z = 0), \quad (3.2)$$

where  $\mu$  runs over five dimensions of the bulk theory.

The Nambu-Goto action is

$$S = -\frac{1}{2\pi\alpha'} \int d\tau d\sigma \mathcal{L} = -\frac{1}{2\pi\alpha'} \int d\tau d\sigma \sqrt{-\det g_{\mu\nu}}, \quad (3.3)$$

where the world-sheet metric  $g_{\mu\nu}$  is the induced metric from background,  $g_{\mu\nu} = G_{MN}\partial_\mu X^M\partial_\nu X^N$  in which  $G_{MN}$  is the five dimensional background. Using the general form of the (3.1) and the rotating string's ansatz (3.2), one can show that the Nambu-Goto Lagrangian density is given by

$$\mathcal{L} = \left[ -G_{uu}(G_{tt} + G_{\psi\psi}\omega^2) - G_{\rho\rho}(G_{tt} + G_{\psi\psi}\omega^2)\rho'^2 - G_{tt}G_{\psi\psi}\theta'^2 \right]^{1/2}. \quad (3.4)$$

Here, the prime denotes a derivative with respect to the holographic radial coordinate  $u$ .

One important feature of this Lagrangian density is  $\theta$  does not appear explicitly in the action and so the momentum conjugate to this field is constant. As we discuss in appendix A, this is not the case for a general rotation in anisotropic background. Then the equation of motion for  $\theta$  is given by

$$\Pi = \frac{\partial \mathcal{L}}{\partial \theta'} = -\frac{G_{tt}G_{\psi\psi}\theta'}{\mathcal{L}} = \text{const.}, \quad (3.5)$$

or equivalently by

$$\theta'^2 = -\Pi^2 \frac{(G_{tt} + G_{\psi\psi}\omega^2)(G_{uu} + G_{\rho\rho}\rho'^2)}{G_{tt}G_{\psi\psi}(G_{tt}G_{\psi\psi} + \Pi^2)}, \quad (3.6)$$

where  $\Pi$  is the momentum conjugate to the angular coordinate  $\psi$ . The LHS of the above equation is positive definite so, the RHS should behave in similar manner. However, the string stretched from the boundary to the horizon and the  $(G_{tt} + G_{\psi\psi}\omega^2)$  term changes the sign in between these points. So, the RHS has a critical point where both numerator and denominator change the sign while the overall sign doesn't change. This critical point is called as  $u_c$  and is defined by

$$G_{tt}(u_c) + G_{\psi\psi}(u_c)\omega^2 = 0, \quad (3.7)$$

$$G_{tt}(u_c)G_{\psi\psi}(u_c) + \Pi^2 = 0. \quad (3.8)$$

which simplifies to

$$|G_{tt}(u_c)| = \Pi \omega, \quad |G_{\psi\psi}(u_c)| = \frac{\Pi}{\omega}. \quad (3.9)$$

For the usual case of an isotropic background which was studied in [17], the geometry is given by

$$ds^2 = \frac{1}{u^2} \left( -(1 - \pi^4 T^4 u^4) dt^2 + d\rho^2 + \rho^2 d\psi^2 + dz^2 + \frac{u^4 du^2}{(1 - \pi^4 T^4 u^4)} \right), \quad (3.10)$$

and (3.7) and (3.8) reduce to

$$u_c = \frac{1}{\pi^2 T^2} \sqrt{-\frac{\Pi \omega}{2} + \frac{1}{2} \sqrt{\Pi^2 \omega^2 + 4\pi^4 T^4}}, \quad (3.11)$$

$$\rho_c = u_c \sqrt{\frac{\Pi}{\omega}}, \quad (3.12)$$

which are the same as the critical values in [17].

We use the following form of the metric components,

$$ds^2 = f(u) (g(u) dt^2 + d\rho^2 + \rho(u)^2 d\psi^2 + h(u) du^2) + G_{zz}(u) dz^2, \quad (3.13)$$

so that the equation of motion for  $\rho$  field can be written in a more compact form. Using this form of the metric (3.13) and the critical equations (3.9), one can find the radius of the rotation at the critical point as

$$\rho_c = \frac{1}{f_c} \sqrt{\frac{\Pi}{\omega}}, \quad (3.14)$$

where  $f_c = f(u_c)$ . Using the equation of motion for  $\theta$  (3.5), one can show the equation of motion for  $\rho(u)$  is given by

$$\begin{aligned} & 2g^2 h^2 (\Pi^2 - \omega^2 f^2 \rho^4) \\ & - [h\rho^3 (-2fg^2 (g + \omega^2 \rho^2) f' + (\Pi^2 \omega^2 - f^2 g^2) g') + g\rho (g + \omega^2 \rho^2) (\Pi^2 + f^2 g \rho^2) h'] \rho' \\ & + 2g^2 h (\Pi^2 - \omega^2 f^2 \rho^4) \rho'^2 \\ & + \rho^3 [2fg^2 (g + \omega^2 \rho^2) f' + (-\Pi^2 \omega^2 + f^2 g^2) g'] \rho'^3 \\ & + 2gh\rho (g + \omega^2 \rho^2) (\Pi^2 + f^2 g \rho^2) \rho'' = 0. \end{aligned} \quad (3.15)$$

To find the radius of rotation at the boundry one needs to solve this equation numerically, even for simple set cases.

The rotating-string solution starts at  $(u = 0, \rho = l)$  passes through the critical point  $(u_c, \rho_c)$  and approaches the black hole horizon located at  $u = u_H$  and a finite value of  $\rho$  that is greater than  $\rho_c$ , which in turn is greater than  $l$ . By expanding (3.15) around  $u_c$ , one can find a series expansion of  $\rho(u)$  as  $\rho(u) = \rho(u_c) + (u - u_c)\rho'(u_c) + \frac{1}{2}(u - u_c)^2 \rho''(u_c) + \dots$ . For example, the first term in expansion  $\rho'(u_c)$  has four solutions

$$\begin{aligned} \rho_c'^{(1,2)} &= \frac{1}{(4f_c g_c^3 \rho_c f_c')} \left[ 4f_c^2 g_c^3 h_c + g_c^3 \rho_c^2 f_c'^2 + \omega^2 g_c^2 \rho_c^4 f_c'^2 + 2f_c g_c^2 \rho_c^2 f_c' g_c' - \Pi^2 g_c'^2 \right. \\ & \left. \pm \left( 16f_c^2 g_c^6 h_c \rho_c^2 f_c'^2 + \left( 4f_c^2 g_c^3 h_c + g_c^3 \rho_c^2 f_c'^2 + \omega^2 g_c^2 \rho_c^4 f_c'^2 + 2f_c g_c^2 \rho_c^2 f_c' g_c' - \Pi^2 g_c'^2 \right)^2 \right)^{1/2} \right], \\ \rho_c'^{(3,4)} &= \pm \sqrt{-h_c}, \end{aligned} \quad (3.16)$$

Obviously, the 3rd and 4th solutions are not physical. The only acceptable solution is the 1st solution (positive sign) which leads to the physical behavior,  $\rho(u=0) = l < \rho_c$ .<sup>6</sup> In principle, once we find the series expansion of  $\rho(u)$  around  $u_c$ , it would be possible to guess the closed form of  $\rho(u)$ . In general it is not easy to find  $\rho(u)$  in this way and the only known result is the simple case of rotating string at zero temperature  $\mathcal{N} = 4$  SYM plasma studied in [31].<sup>7</sup>

We use numerical methods to find the shape of the rotating string. Given angular momentum  $\omega$  and constant of motion  $\Pi$ , one finds  $(u_c, \rho_c)$  point from (3.9) and (3.14). But there is a problem at this point, the equation of motion (3.15) (and the Lagrangian (3.4)) is singular at the critical point. So, by starting from this point, one can not find the numerical solution for the equation of motion of  $\rho$  (3.15).<sup>8</sup> Fortunately this problem appears only at one point and we can use the equation of motion (3.15) and expand it up to any order that we want. Since the equation (3.15) is a second order differential equation, we must know two boundary conditions to find the solution uniquely. We can find the second derivative of the  $\rho(u)$  at  $u_c$ ,  $\rho''(u_c)$  and then solve the equation numerically by expanding from  $u_c - \epsilon$  ( $u_c + \epsilon$ ) to the boundary (horizon).

In general, the energy loss rate of the world-sheet is given by

$$\frac{dE}{dt} = \Pi_t^\sigma = -\frac{\delta S}{\delta(\partial_\sigma X^0)}, \quad (3.17)$$

In our case, by using equations (3.4), (3.5) and (3.9), one can show that there are some different expansions for the rate of energy loss which are very useful,

$$\frac{dE}{dt} = -\frac{G_{tt}G_{\phi\phi}\omega\theta'}{2\pi\alpha'\mathcal{L}} = \frac{\Pi\omega}{2\pi\alpha'} = \frac{|G_{tt}(u_c)|}{2\pi\alpha'}. \quad (3.18)$$

In appendix B we will show that the general formula for the rate of energy loss for a string moving on a line is the same as the last equality in the above equation. The difference is a different value for the critical point of the radial holographic coordinate,  $u_c$ .

To find and investigate the solution in terms of the parameters of the boundary theory, we will focus on the strongly-coupled anisotropic plasma in the next section and compare our results with the rotating string in the isotropic background which is the  $\text{AdS}_5 \times \text{S}^5$  theory with  $\mathcal{N} = 4$  SYM theory on the boundary. Then, we will compare the energy loss of a rotating string to the drag force in the strongly-coupled anisotropic plasma studied in [21, 22] and the radiation results on isotropic case investigated in [17].

## 4 Rotating string in strongly-coupled anisotropic plasma

To study the energy loss of the rotating quark in strongly-coupled anisotropic plasma, one should solve equation (3.15) to find the radius function  $\rho(u)$ . The general behavior of the angular function,  $\theta(u)$ , is the same as in the isotropic case studied in [17], so we are not going to find the angle function  $\theta(u)$ , which has no effect on energy lost.

<sup>6</sup>In most of the case  $f(u) \propto u^n$  which leads to a positive (negative) solution of  $\rho'_c$  for  $n > 0$  ( $n < 0$ ).

<sup>7</sup>K.B.F thanks D.Nickel for discussion on this point.

<sup>8</sup>This challenge have been seen also in some other calculation [32] in a range of  $u$  and, it leads to using the Polyakov action instead of Nambu-Goto action.

Valuable results are the comparison of the anisotropic case with the isotropic background at the same temperature or at the same entropy density. We do these comparisons both for the gravity side (bulk) and the field theory side (boundary) of the AdS/CFT correspondence.

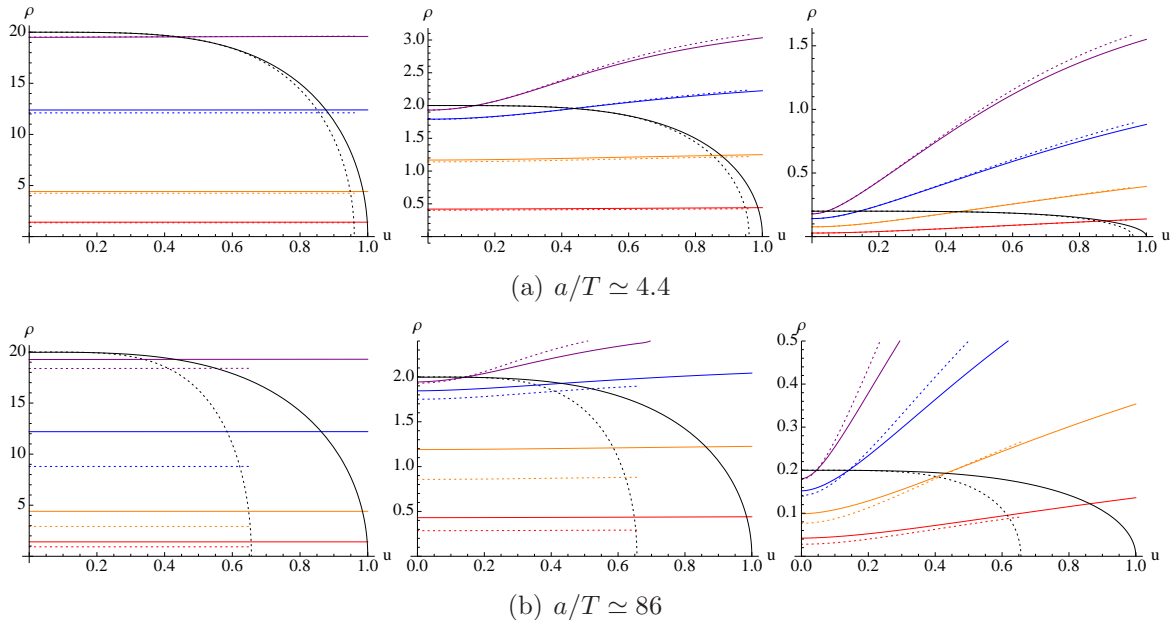


Figure 2: The radial dependence  $\rho(u)$  of spiraling string hanging down from rotating quarks in anisotropic (solid curves) and isotropic (dotted curves) media for various different choices of parameters:  $\omega = 0.05, \omega = 0.5$  and  $\omega = 5.0$  from left to right, and the set of values for the constant of motion  $\Pi = 0.1$  (red), 1 (orange), 10 (blue), 100 (purple) for all of the figures. In (a) and (b), the anisotropic parameter is specified as  $a/T \simeq 4.4$  and  $a/T \simeq 86$ , respectively. This comparison with the isotropic plasma has been done at the same temperature.

By assumption, the temperature and the entropy density of the two sides of the AdS/CFT correspondence are the same. Therefore it's enough to find these parameters for the gravity side by using simple definitions of the temperature and entropy density. We will study the energy loss of a rotating quark in an anisotropic plasma by comparing the results with the isotropic case both with the same temperature and with the same entropy.

Plugging the anisotropic background (2.1) into the critical equation (3.9), the equation of motion for  $\rho(u)$  (3.15), and the equation which determines the  $\rho'_c$ ; one can reduce these equations to a simpler form. As we mentioned in section 3, to find numerical results for  $\rho(u)$  we should integrate from  $u_c - \epsilon$  ( $u_c + \epsilon$ ) to the boundary (horizon).

In Fig.2, we compare the anisotropic plasma (solid curves) with isotropic plasma (dotted curves) in the same temperature. These plots show the radial dependence  $\rho(u)$  of a spiraling string hanging down from rotating quarks for different angular velocities:  $\omega = 0.05, 0.5, 5.0$ , from left to right. In this figure the constant of motion (angular momenta) is given by  $\Pi = 0.1$  (red), 1 (orange), 10 (blue), 100 (purple). The effect of anisotropy is given by the ratio of anisotropic parameter to the temperature  $a/T \simeq 4.4$  (a) and  $a/T \simeq 86$  (b). Note that the string is not going into the horizon so the dotted (solid) curves finished at the horizon of isotropic (anisotropic) solutions.

On the other hand, for fixed  $\omega$  and  $\Pi$ , which means the role of energy loss is fixed, the

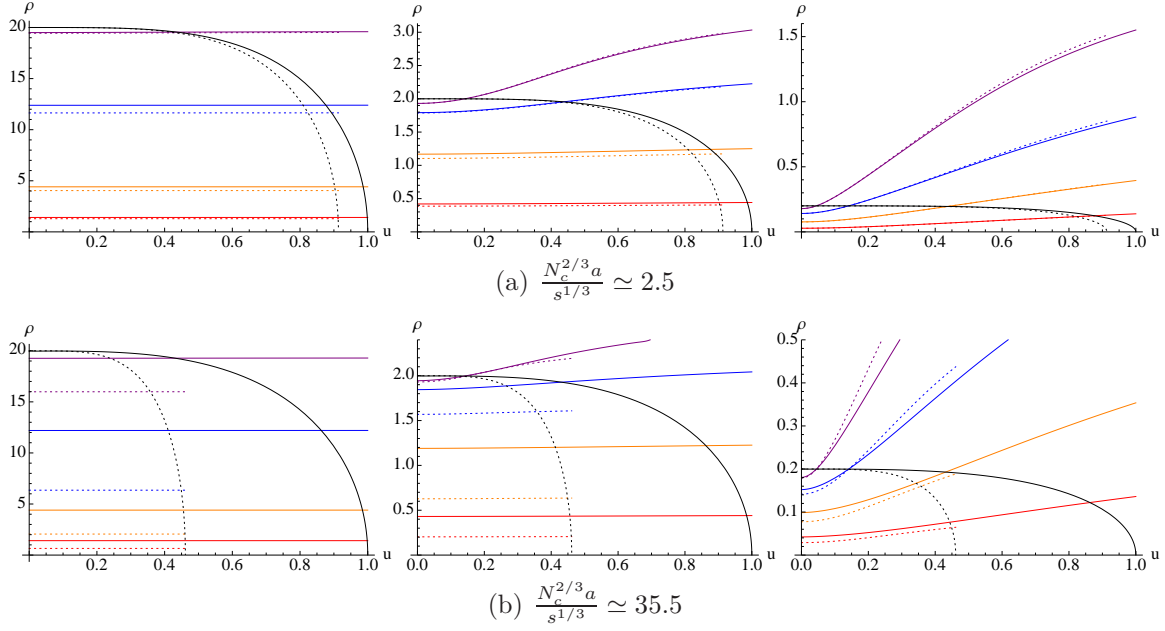


Figure 3: The radial dependence  $\rho(u)$  of spiraling string hanging down from rotating quarks in anisotropic (solid curves) and isotropic (dotted curves) media for various different choices of parameters:  $\omega = 0.05, \omega = 0.5$  and  $\omega = 5.0$  from left to right, and the set of values for the constant of motion  $\Pi = 0.1$  (red), 1 (orange), 10 (blue), 100 (purple) for all of the figures. In (a) and (b), the anisotropic parameter is specified as  $\frac{N_c^{2/3} a}{s^{1/3}} \simeq 2.5$  and 35.5, respectively. This comparison with the isotropic plasma has been done at the same entropy.

bigger radius of rotation on the boundary means a larger velocity for the quark.

We summarize the important results of the plots as follows:

- The anisotropy mainly effected the shape of the spiraling string. It is easy to see that by increasing the anisotropy the radius of rotation significantly changes.
- While in most of the cases the radius of rotation on the boundary in anisotropic cases is larger than isotropic cases, for small anisotropy,  $a/T \simeq 4.4$ , and small angular velocity,  $\omega = 0.05$ , this is not the case.
- For the fixed  $\omega$  and  $\Pi$ , the radius on the boundary is bigger than in the isotropic case which means a larger velocity of the quark in the field theory. Using the energy loss relation (3.18),  $\frac{dE}{dt} \propto \Pi\omega$ , one can show that for the same velocity  $v$  and the same angular velocity  $\omega$  the energy loss in the anisotropic plasma is less than the energy loss in the isotropic case (except for the small  $\omega$  and large  $v$  which is similar to the drag force [21]). We will discuss this point in the later sections.
- For the case of small  $\omega$  (0.05), the isotropic and anisotropic curves with the same  $\Pi$  do not cross each other and each curve is almost straight. So the energy loss should be very similar to the drag force and effect of radiation is very small. We will show (both numerically and analytically) that this is the case.
- For a bigger  $\omega$  (0.5) the curves cross each other for enough large  $\Pi$ 's. We will see that that this crossing may be assumed to be a measure for interplay between the linear drag channel and the radiation channel of energy loss.

- In large  $\omega$  (5.0), for small  $a/T$  the radius on the horizon is smaller than the isotropic case and there is no crossing. But for large anisotropy the curves cross each other and the radius on the horizon is larger than isotropic case, both for small and large anisotropy.

In Fig.3, we show the results for the same entropy density. The general behavior of the plots are similar to the plots we find for the same temperature cases in Fig.2. The main difference is for small  $a/T$ , there is no strange behavior as like as the same temperature cases we discussed earlier. So the radius of rotation on the boundary in anisotropic plasma is smaller than isotropic case for fixed  $\omega$  and  $\Pi$  in both small and large anisotropy. Again, we specified the anisotropic results by solid curves and the isotropic plasma by dotted curves,  $\omega = 0.05, 0.5, 5.0$  from left to right and  $\Pi = 0.1$  (red), 1 (orange), 10 (blue), 100 (purple).

Here we compare the rotating string in anisotropic and isotropic cases with fixed  $\Pi$  and  $\omega$ , which means the fixed energy loss rate by using eq.(3.18). We investigate this comparison from two different point of views: gravity theory and boundary theory. The parameters of solutions from gravity point of view are  $\omega$  and  $\Pi$  but, from boundary theory they are  $\omega$  and  $v = l\omega$ . Therefore from gravity point of view we find the ratio of energy loss in anisotropic and isotropic plasmas as a functions of  $\Pi$ , and from boundary theory point of view we find this ratio as a functions of  $v$ .

## 4.1 The energy loss

In this section, we study the energy loss of a heavy test quark. Plugging the anisotropic background metric (2.1) into the general formula for the rate of energy loss (3.18) one can show that

$$\frac{dE}{dt} = \frac{\Pi \omega}{2\pi\alpha'} = \frac{1}{2\pi\alpha'} \frac{\mathcal{F}_c \mathcal{B}_c}{u_c}, \quad (4.1)$$

where  $\mathcal{F}_c$  and  $\mathcal{B}_c$  are the value of these functions at the critical point  $(u_c, \rho_c)$  which is defined by

$$\frac{\mathcal{F}_c \mathcal{B}_c}{u_c^2} = \Pi\omega, \quad \rho_c = u_c \sqrt{\frac{\Pi}{\omega}} \quad (4.2)$$

Therefore, from bulk point of view, the energy loss just depends on the value of  $u_c$  which is a function of  $\Pi$  and  $\omega$  via equations (4.2).

Using (4.1), it is straightforward, using the numerical techniques described before, to evaluate the energy loss for a quark moving in a circle with angular frequency  $\omega$  as a function of radius  $l$  (or equivalently as a function of velocity of the quark  $v = l\omega$ ).

From the bulk point of view, we pick an  $\omega$  and a series of values of  $\Pi$ . For each  $\Pi$ , we obtain the corresponding string world-sheet. From that solution, one finds that the energy loss of the quark increases without bound as  $l$  approaches to  $1/\omega$ , which is the radius at which the quark would be moving at the speed of light. We call the radius of the rotating quark in the anisotropic and isotropic medium  $l_{aniso}$  and  $l_{iso}$ , respectively.

The radius of the rotation on the boundary (or the velocity of the rotating quark  $v = l\omega$ ) is a monotonic increasing function of  $\Pi$  for fixed  $\omega$  in both isotropic and anisotropic backgrounds. As an example, we plot the velocity of the quark as a function of  $\Pi$  for  $\omega = 5.0$  and  $a/T \simeq 86$  in Fig.4. This behavior is general for any value of  $\omega$  and  $a/T$  and it will be extremely useful in what follows.

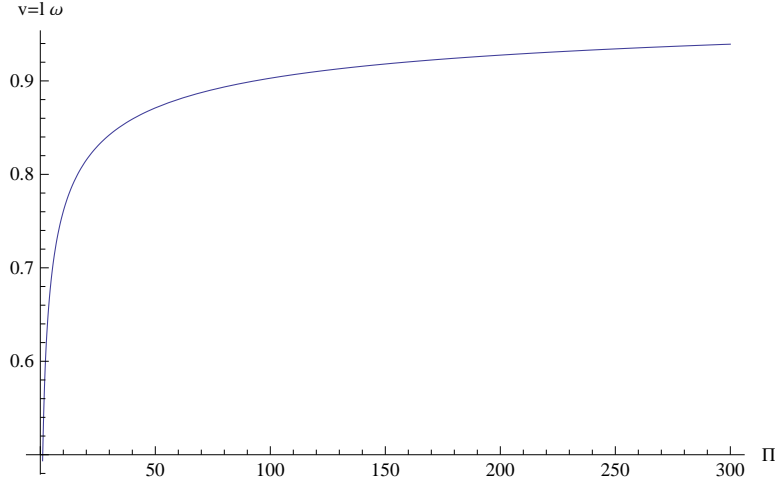


Figure 4: In general for both isotropic and anisotropic solutions the velocity (or equivalently the radius of the rotation) of the end point of the string on the boundary is a monotonically increasing function of  $\Pi$ . As an example, in this plot we show the velocity of the quark at the boundary versus the constant of motion  $\Pi$  for  $\omega = 5.0$  and  $a/T \simeq 86$ .

We plot  $l_{aniso}/l_{iso}$  (which is as same as  $v_{an}/v_{is}$ ) as a function of the constant of motion  $\Pi$  for different angular velocities,  $\omega$  and different  $a/T$  for the same temperature and the same entropy in figures 5 and 6, respectively. Each figure contains the plots for four anisotropic parameters  $a/T \simeq 0.78, 4.4, 25, 86$  and three angular velocities  $\omega = 0.05$  (red),  $0.5$  (green),  $5.0$  (black).

There are two general features in all plots:

$$(1) \quad l_{aniso} > l_{iso}|_{\Pi \rightarrow 0}, \quad (2) \quad l_{aniso} \simeq l_{iso}|_{\Pi \rightarrow \infty}. \quad (4.3)$$

This shows that, for large enough  $\Pi$ 's the quark can not see the anisotropy while, the anisotropy has a significant affect on the rotating quark for smaller  $\Pi$ 's. We will discuss about this behavior also from boundary theory point of view.

In Fig.5, it is clearly seen that for the same temperature cases, there is a minimum value, which is less than 1, for this ratio in small angular velocity,  $\omega = 0.05$ , and small anisotropy,  $a/T (\simeq 0.78 \text{ and } 4.4)$ . This minimum disappear by increasing the angular velocity and/or  $a/T$ . But all plots with the same entropy in Fig.6 show that  $l_{aniso}$  is bigger than  $l_{iso}$  for any  $\omega$  and  $\Pi$ .

According to the first equality in equation (4.1), the energy loss rate is proportional to  $\Pi\omega$ . On the other hand, in both isotropic and anisotropic cases the radii of rotation at the boundary are monotonically increasing with respect to  $\Pi$  (e.g. Fig. 4). So from the boundary theory point of view, one can conclude that for  $l_{aniso}/l_{iso} > 1$  ( $l_{aniso}/l_{iso} < 1$ ) the rate of energy loss in an anisotropic plasma is smaller (larger) than the isotropic case, for fixed  $v$  and  $\omega$ . It is easy to see that in these conditions the rate of energy loss in an anisotropic plasma is less than isotropic case in general except for the small value of  $\omega(0.05)$  and small  $a/T(\simeq 0.78)$ . In this case for large enough  $\Pi(\gtrsim 40)$ , corresponding to  $v \simeq 0.9$ , the energy loss rate in the anisotropic plasma is more than the isotropic case. This is in perfect agreement with the drag force results [21, 22]. We expect that for a small angular velocity the dominant part of the energy loss is due to the drag force, and the above agreement bolsters this idea. We checked this behavior for a range of  $a/T$  and we see that

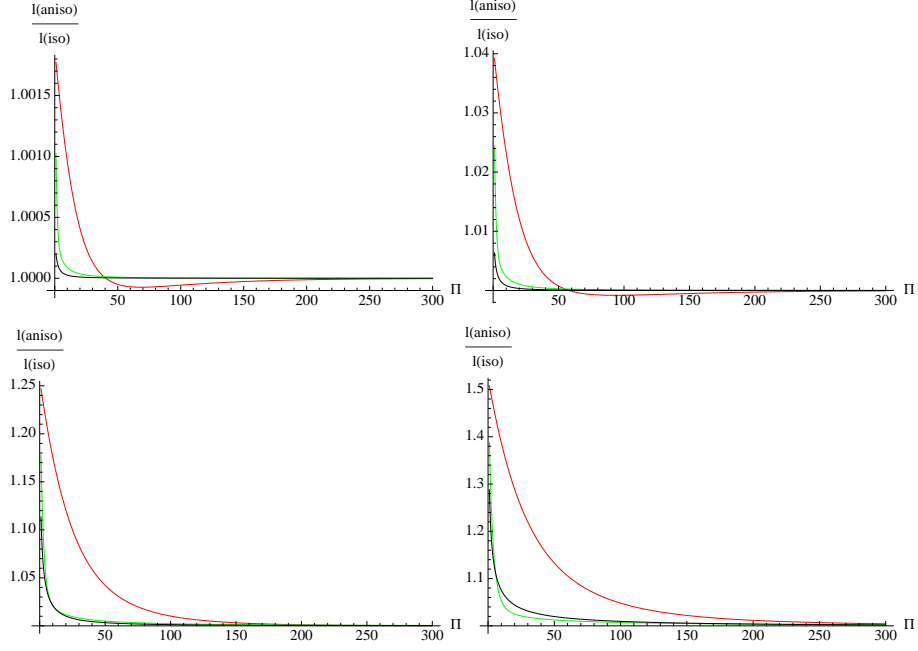


Figure 5: The ratio of the radius of rotating quark in an anisotropic medium to the isotropic case as a function of the constant of motion  $\Pi$ . This comparison has been done for the same temperature. In each plot of this figure, the angular velocity is  $\omega = 0.05$  (red),  $0.5$  (green),  $5.0$  (black), and  $a/T \simeq 0.78$  (top-left),  $4.4$ (top-right),  $25$ (down-left),  $86$ (down-right)

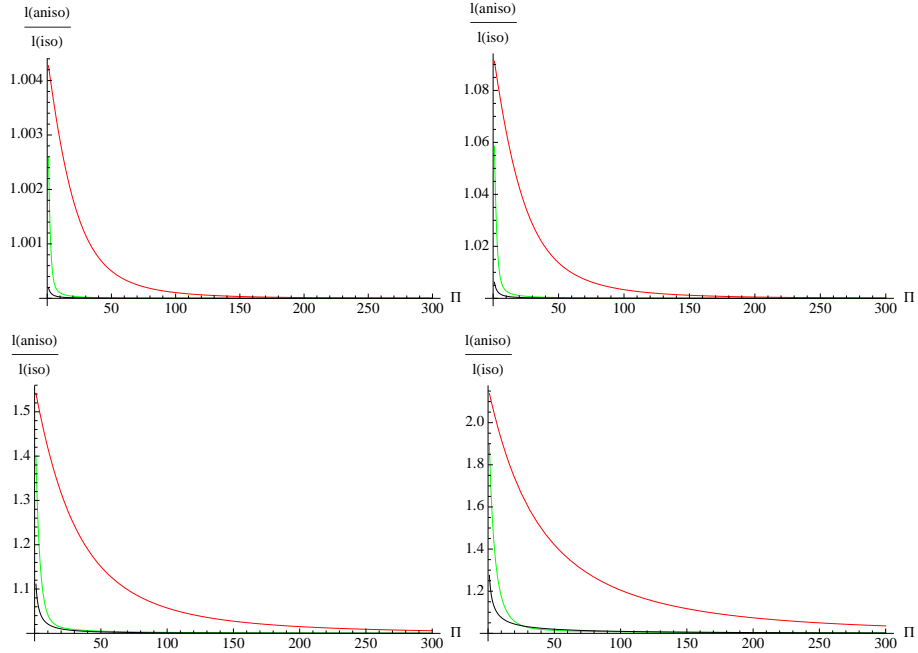


Figure 6: The ratio of the radius of rotating quark in an anisotropic medium to the isotropic case as a function of the constant of motion  $\Pi$ . This comparison has been done for the same entropy. In each plot of this figure, angular velocity is  $\omega = 0.05$  (red),  $0.5$  (green),  $5.0$  (black), and  $\frac{N_c^2/3 a}{s^{1/3}} \simeq 0.46$  (top-left),  $2.5$  (top-right),  $12$ (down-left),  $35.5$  (down-right)

this happens for  $a/T \lesssim 12$ .

From the boundary theory point of view, to compare the energy loss in two different media it is natural to fix the velocity,  $v = l\omega$ . The ratios of the energy loss rate in anisotropic background to the isotropic case as a function of the velocity of the rotating quark are given in Fig.7. These plots are our main outputs and in following sections we will investigate these results both analytically and numerically.

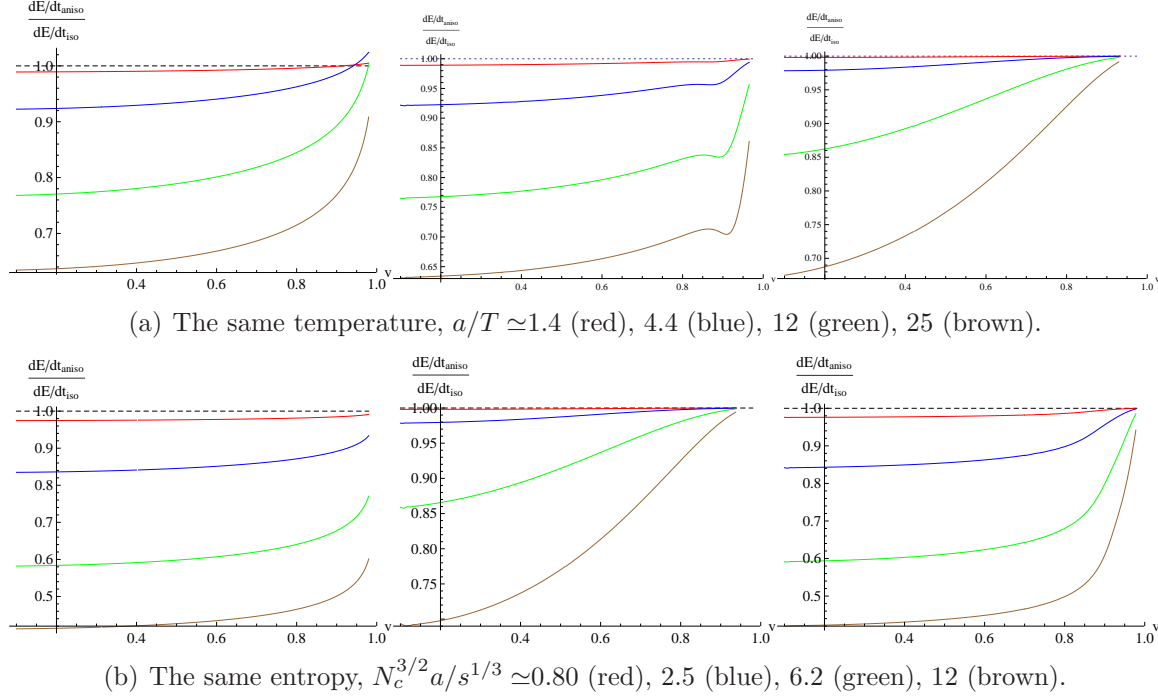


Figure 7: The ratio of the energy loss in anisotropic backgrounds to the isotropic cases for different angular velocities:  $\omega = 0.05, 0.5, 5.0$  from left to right.

We summarize the important features of the plots in Fig.7 as follows:

- Again one can see that the ultra-relativistic quark (or large  $\Pi$  from gravity point of view) can not see the anisotropy in terms of its energy loss rate, except for small anisotropy and small angular velocity and the same temperature case. As expected, this is very similar to the drag force studied in [21].
- The ratios of energy loss rates are monotonic functions, except for  $\omega = 0.5$  and large enough  $a/T$  and the same temperature. In this exception one can see a competition for energy loss between the linear drag and the radiation channels. We will discuss this point later.
- For fixed velocity  $v$  and anisotropy the bigger angular velocity  $\omega$  leads to the smaller ratio of energy loss rate, except for large velocity which breaks for medium  $\omega$ .

One should note that the linear drag is a function of velocity of the quark while, the radiation is a function of angular acceleration,  $\hat{a} = v\omega$ . Since  $v \leq 1$ , small enough  $\omega$  leads to small  $\hat{a}$  and small radiation for any velocity. Therefore for small  $\omega$  the dominant part of the energy loss is due to the drag force. One interesting situation is for intermediate  $\omega$ . In this case for small  $v$  the drag force is dominant while for large enough  $v$ ,  $\hat{a}$  is large enough

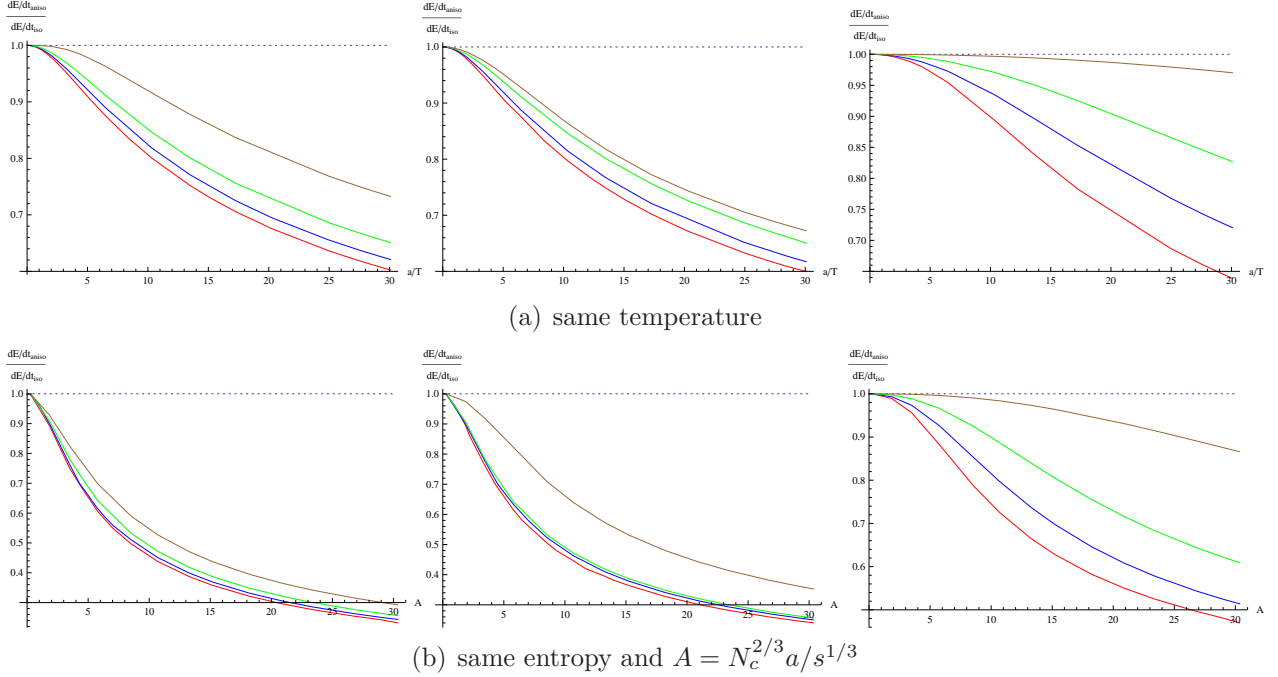


Figure 8: Energy loss of rotating quark as a function of anisotropy at the same temperature (a) or at the same entropy density (b) for four different velocities  $v = 0.2, 0.5, 0.7, 0.9$ , from bottom to top in each plot. In each row, angular velocities are  $\omega = 0.05, \omega = 0.5$  and  $\omega = 5.0$  from left to right.

and there is a competition for energy loss between drag and radiation. As one can see in Fig.7, this is an interesting part for the energy loss of a quark in this anisotropic plasma model.

We studied the shape of rotating string in an anisotropic background and the rate of energy loss of a rotating quark in the dual anisotropic plasma, by using AdS/CFT correspondence, for some specific values of anisotropy. In Fig. 8, we show the ratio of energy loss rate of anisotropic to isotropic plasmas as function of  $a/T$  for four velocities. The first row is for the same temperature cases and the second row is for the same entropy density and in each row the angular velocity is  $\omega = 0.05, 0.5, 5.0$  from left to right. From these plots it is obvious that the rate of energy loss in anisotropic background is smaller than the isotropic case and for fixed  $v$  and  $\omega$  the larger anisotropy leads to the smaller rate of energy loss. This is the case both in the same temperature and the same entropy cases.

It would be very interesting to ask about mechanism of energy loss in two plasmas, is it drag force or radiation? In section 6, by comparing the results with both linear drag and synchrotron radiation, we will show that the anisotropy decreases the radiation when the parton propagates perpendicular to the direction of the anisotropy. This is in perfect agreement with result of [33].

## 5 Analytic limits

In this section, we consider two different limits in which we can do some analytical calculations, ultra-relativistic limit and small  $a/T$  limit. For these cases we know the metric functions of dual gravity (2.1) explicitly [20] and we can get some analytical results to

justify our numeric results at least in these limits. The results also show that the energy loss rate depend on the temperature (or horizon radius) and  $a/T$ , as expected from the discussion at the end of section 2.

## 5.1 Ultra-relativistic limit

There are two different options for an ultra-relativistic limit,

- Large but fixed  $v = l\omega = \text{const.}$ ,  $\hat{\alpha} = v\omega \rightarrow 0$ , meaning  $\omega \rightarrow 0$
- Large but fixed  $v = l\omega = \text{const.}$ ,  $\hat{\alpha} = v\omega \rightarrow \infty$ , meaning  $\omega \rightarrow \infty$

For the second case, as we see in Fig.2 and Fig.3, the critical point  $u_c$  can be anywhere between the horizon  $u = u_H$  and the boundary  $u = 0$ . For this case which is completely general we know nothing analytically. But for the first case the critical point  $u_c$  approaches to the boundary  $u_c \rightarrow 0$ ,<sup>9</sup> which is similar to the drag force in the large velocity limit  $v \rightarrow 1$  [21]. Therefore one can use the near boundary expansion of metric functions [20],

$$\begin{aligned}\mathcal{F} &= 1 + \frac{11a^2}{24}u^2 + \left(\mathcal{F}_4 + \frac{7a^4}{12}\log u\right)u^4 + \mathcal{O}(u^6), \\ \mathcal{H} &= 1 + \frac{a^2}{4}u^2 - \left(\frac{2\mathcal{B}_4}{7} - \frac{5a^4}{4032} - \frac{a^4}{6}\log u\right)u^4 + \mathcal{O}(u^6), \\ \mathcal{B} &= 1 - \frac{11a^2}{24}u^2 + \left(\mathcal{B}_4 - \frac{7a^4}{12}\log u\right)u^4 + \mathcal{O}(u^6),\end{aligned}\tag{5.1}$$

where  $\mathcal{F}_4$  and  $\mathcal{B}_4$  depend on  $a$ ,  $T$  and a conformal anomaly scale, but they are not determined by the near boundary analysis [20].

To find the critical point  $(u_c, \rho_c)$  for this case, we solve the equations (4.2) analytically using the above expansion of metric functions (5.1). The second equation in (4.2) simplifies to

$$\Pi\omega = \frac{v_c^2}{u_c^2},\tag{5.2}$$

where  $v_c \equiv \rho_c\omega$  is the velocity of the string at the critical point,  $u_c$ . Note that in this limit the radius of the rotating string on the boundary,  $l$ , is very close to the radius of the string at the critical point,  $\rho_c$ , Fig.2 and Fig.3. Therefore the velocity of the string at these two points are also very close to each other. By using this point, we can find the value of  $u_c$  by solving the first equation in (4.2) to leading order in  $1 - v_c^2$ ,

$$\frac{1}{u_c^2} = \frac{T^2}{\sqrt{1 - v_c^2}}\Xi, \quad \Xi = \sqrt{\frac{121a^4}{576T^4} - \frac{\mathcal{F}_4 + \mathcal{B}_4}{T^4}}\tag{5.3}$$

which is the same expansion for the critical point found for the drag force calculation [21]. But we should remind that  $v_c$  is a function of  $u_c$  via eq.(5.2) so the explicit relation for  $u_c$  is given by

$$u_c = \frac{1}{\Xi T^2} \sqrt{-\frac{\Pi\omega}{2} + \frac{1}{2}\sqrt{\Pi^2\omega^2 + 4\Xi^2 T^4}},\tag{5.4}$$

---

<sup>9</sup>From Fig.2 and Fig.3, it is easy to see that for fixed  $\omega$ , a larger velocity correspond to a larger radius of rotation at the boundary which leads to a larger  $\Pi$  and a smaller  $u_c$ .

Note that the energy loss rate is given by the time component of the background metric at the critical point,  $|G_{tt}(u_c)|$  eq.(3.18) and is given by

$$\left. \frac{dE}{dt} \right|_{aniso} = \frac{\sqrt{\lambda} T^2}{2\pi} \frac{v_c^2}{\sqrt{1-v_c^2}} \sqrt{\frac{121a^4}{576T^4} - \frac{\mathcal{F}_4 + \mathcal{B}_4}{T^4}}. \quad (5.5)$$

Again, this is exactly the same results which was found for the linear drag in [21].

For the linear drag, there is only one velocity for all of the points of string but in our case the velocity is the velocity of the critical point of the string,  $v_c$ . As it is shown in Fig.9 for small enough  $v$ , corresponds to small enough  $\Pi$ , for  $\omega = 0.05$  and  $\omega = 0.5$  the dominant part of the energy loss is due to the linear drag. But the validity for this approximation is not just  $\hat{\alpha} \rightarrow 0$ . As one can see in Figs.2 and 3 for large  $\Pi$  the radii of rotating string on the boundary  $u = 0$  and the critical point  $u_c$  are very close to each other while, the rest of the string below the critical point has larger radius. Therefore, the  $v \simeq v_c$  approximation is not valid any more for all of the string points. This limit is discussed in [17] for the isotropic plasma as well.

Since the the energy loss rate (5.5) is the same as the linear drag results given in [21] and its validity range is as same as isotropic case, it's clear that the comparison between the energy loss rate in the anisotropic and in the isotropic backgrounds leads to the same results found for the drag force in [21]. Remind that this is true just in special limit, large and fixed  $v = l\omega$ ,  $\omega \rightarrow 0$  and small enough  $l$ .

For small and large  $a/T$  limits the  $\mathcal{F}_4$  and  $\mathcal{B}_4$  parameters are known [20] and one can find more explicit results. For small  $a/T$ ,

$$\begin{aligned} \mathcal{F}_4 &= -\pi^4 T^4 - \frac{9\pi^2 T^2}{16} a^2 - \left[ \frac{101}{384} - \frac{7}{12} \log\left(\frac{2\pi T}{a}\right) - \frac{7}{12} \log\left(\frac{a}{\Lambda}\right) \right] a^4 + \mathcal{O}(a^6), \\ \mathcal{B}_4 &= \frac{7\pi^2 T^2}{16} a^2 + \left[ \frac{593}{1152} - \frac{7}{12} \log\left(\frac{2\pi T}{a}\right) - \frac{7}{12} \log\left(\frac{a}{\Lambda}\right) \right] a^4 + \mathcal{O}(a^6), \end{aligned} \quad (5.6)$$

where  $\Lambda$  relates to the conformal anomaly scale. It is easy to see that the ratio of the energy loss in the anisotropic plasma to the the energy loss in the isotropic case doesn't depend on parameter  $\Lambda$ . For the same temperature, one can show that this ratio is given by

$$\left. \frac{dE/dt_{aniso}}{dE/dt_{iso}} \right|_{temp} = 1 + \frac{a^2}{16\pi^2 T^2} + \mathcal{O}\left(\frac{a^4}{T^4}\right). \quad (5.7)$$

Therefore the energy loss rate of ultra-relativistic quark rotating uniformly in transverse direction plane in an anisotropic plasma with small  $a/T$ , small  $\omega$  and large but fixed  $v$  is greater than the isotropic case at equal temperatures. This is similar to the drag force results for small  $a/T$  and large but fixed  $v$  [21]. This analytic result is in agreement with our numerical results given in Fig.5 (red curves in the first row plots) and Fig.7 (red and blue curves in the top-left plot) .

To compare the results for equal entropy density, we use the relation between entropy density and temperature for an anisotropic plasma in small  $a/T$  [20]

$$s = \frac{\pi^2 N_c^2 T^3}{2} + \frac{N_c^2 T}{16} a^2 + \mathcal{O}\left(\frac{a^4}{T^4}\right), \quad (5.8)$$

which causes to different ratio for the rate of energy loss for the same entropy densities,

$$\left. \frac{dE/dt_{aniso}}{dE/dt_{iso}} \right|_{\text{entropy}} = 1 - \frac{N_c^{4/3}}{48(2\pi)^{3/2}} \left( \frac{a}{s^{1/3}} \right)^2 + \mathcal{O} \left( \frac{a^4}{s^{4/3}} \right). \quad (5.9)$$

Again, it is similar to the drag force results and the energy loss rate in the anisotropic plasma is smaller than the isotropic case at equal entropy density. These analytic results are in agreement with our numerical results given in Fig.6 (red curves in the first row plots) and Fig.7 (red and blue curves in the down-left plot) .

As expected, for large  $a/T$  the results are the same as the linear drag and the energy loss in the anisotropic plasma is always greater than the energy loss in the isotropic case both for equal temperatures and equal entropy densities. Using the explicit relations for  $\mathcal{F}_4$  and  $\mathcal{B}_4$  parameters [20]

$$\mathcal{F}_4 = \frac{1}{132} \left[ 132a^4 c_{\text{int}} + 77a^4 \log \left( \frac{a}{\Lambda} \right) - 384c_{\text{ent}} \pi^2 a^{1/3} T^{11/3} + \dots \right], \quad (5.10)$$

$$\mathcal{B}_4 = \frac{1}{6336} \left[ 1331a^4 - 6336a^4 c_{\text{int}} - 3696a^4 \log \left( \frac{a}{\Lambda} \right) + 4032c_{\text{ent}} \pi^2 a^{1/3} T^{11/3} + \dots \right], \quad (5.11)$$

the ratio of the energy loss rate in the anisotropic plasma to the energy loss rate in the isotropic case is given by

$$\left. \frac{dE/dt_{aniso}}{dE/dt_{iso}} \right|_{\text{temp}} = \frac{\sqrt{2c_{\text{ent}}}}{\pi} \left( \frac{a}{T} \right)^{1/3} + \dots, \quad (5.12)$$

$$\left. \frac{dE/dt_{aniso}}{dE/dt_{iso}} \right|_{\text{entropy}} = \frac{1}{2^{1/6} \pi^{1/3} c_{\text{ent}}^{3/16} N_c^{1/24}} \left( \frac{s^{1/3}}{a} \right)^{1/16} + \dots, \quad (5.13)$$

for equal temperatures and equal entropy densities, respectively.  $c_{\text{ent}}$  is a constant introduced in the entropy density in section 2 and  $c_{\text{int}}$  is an integration constant introduced in [20]. As expected, this is again the same results as drag force [21].

## 5.2 Small $a/T$ limit

For small  $a/T$  the metric functions and the radius of the horizon are known as some expansions around the black D3-brane solution [20],

$$\begin{aligned} \mathcal{F} &= 1 - \frac{u^4}{u_H^4} + a^2 \mathcal{F}_2 + \mathcal{O}(a^4), \\ \mathcal{B} &= 1 + a^2 \mathcal{B}_2 + \mathcal{O}(a^4), \\ \log \mathcal{H} &= \frac{a^2 u_H^2}{4} \log \left( 1 + \frac{u^2}{u_H^2} \right) + \mathcal{O}(a^4), \\ u_H &= \frac{1}{\pi T} + \frac{5 \log 2 - 2}{48\pi^3 T^3} a^2 + \mathcal{O}(a^4), \end{aligned} \quad (5.14)$$

in which

$$\mathcal{F}_2 = \frac{1}{24u_H^2} \left[ 8u^2(u_H^2 - u^2) - 10u^4 \log 2 + 3u_H^4 + 7 \log \left( 1 + \frac{u^2}{u_H^2} \right) \right], \quad (5.15)$$

$$\mathcal{B}_2 = -\frac{u_H^2}{24} \left[ \frac{10u^2}{u_H^2 + u^2} + \log \left( 1 + \frac{u^2}{u_H^2} \right) \right]. \quad (5.16)$$

It is easy to find the critical point by using the general formula (3.9) and above expansions for the background metric. Obviously, the result is an expansion around the isotropic critical point (3.11). Up to second order in  $a$  the critical point is given by

$$u_c = u_{\text{iso}} + a^2 u_c^{(2)} + \mathcal{O}(a^4), \quad \rho_c = u_c \sqrt{\frac{\Pi}{\omega}}, \quad (5.17)$$

where

$$u_{\text{iso}} = \frac{1}{\pi^2 T^2} \sqrt{-\frac{\Pi\omega}{2} + \frac{1}{2} \sqrt{\Pi^2 \omega^2 + 4\pi^4 T^4}}, \quad (5.18)$$

Doing some calculations it is easy to show that the first correction to the isotropic critical point is

$$u_c^{(2)} = \frac{3 - 2\pi^2 T^2 u_{\text{iso}}^2 (1 + \pi^2 T^2 u_{\text{iso}}^2) + (-1 + 8\pi^4 T^4 u_{\text{iso}}^4) \log(1 + \pi^2 T^2 u_{\text{iso}}^2)}{48\pi^2 T^2 u_{\text{iso}} (2\pi^4 T^4 u_{\text{iso}}^2 + \Pi\omega)}. \quad (5.19)$$

In contrast to the ultra-relativistic limit studied in the previous subsection, one can not find the analytic results from boundary theory point of view. It's because, there is no analytic relation between the radius of rotation at the critical point  $\rho_c$  and the radius of rotation at the boundary  $l$ , which is the case for ultra-relativistic limit (see the discussion after eq.(5.2)). Therefore to explain every thing from boundary theory point of view we must solve the general equation of motion for  $\rho$  (3.15) numerically from critical point to the boundary by using the explicit metric functions (5.14) and the explicit relation for the critical point (5.17). The results are in perfect agreement with the results we found numerically for small  $a/T$  in previous section and since there is no more point we don't show the plots here.

## 6 Comparison with the linear drag and the synchrotron radiation

In this section we compare our results of the rate of energy loss for a rotating quark in an anisotropic plasma with two different known cases, the linear drag and the synchrotron radiation. First we want to compare the energy loss rate of rotating quark with the energy loss rate in the linear drag case. The drag force experienced by an infinitely massive quark propagating at constant velocity through an anisotropic, strongly-coupled  $\mathcal{N} = 4$  SYM plasma was studied in [21, 22]. In Fig.9 we show the ratio of the total energy loss rate of rotating quark to its linear drag part as a function of velocity of the quark in the boundary theory for different  $\omega$  and different  $a/T$ .

As expected, for small  $\omega$  the dominant part of the ratio of energy loss is due to the linear drag for a wide range of velocity of the quark on the boundary. In this range, the local velocity of the rotating string at each point can be approximated by the velocity of the quark at the boundary which means the string behaves similar to the linear drag case studied in [21, 22].

In this limit we show a perfect agreement between the energy loss rate of rotating quark and the linear drag analytically. The rate of energy loss for a rotating string is given by (3.18) or equivalently by

$$\frac{dE}{dt} = \frac{\Pi\omega}{2\pi\alpha'} = \frac{\Pi v_c}{2\pi\alpha' l}. \quad (6.1)$$

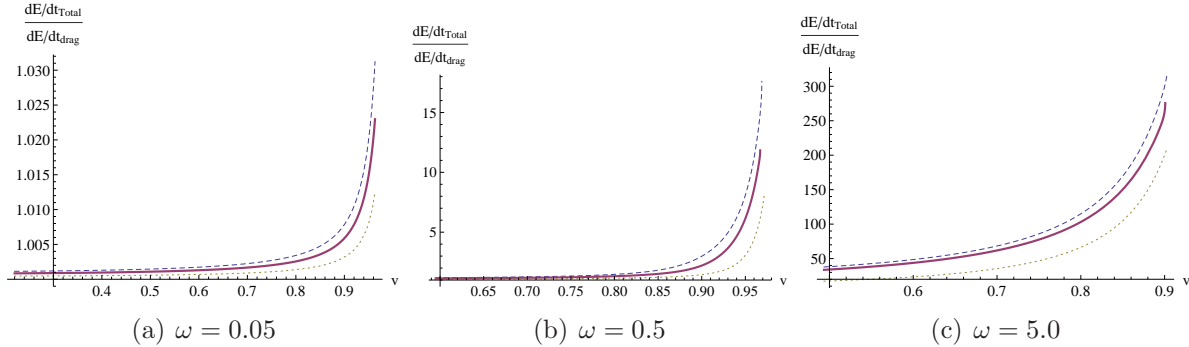


Figure 9: The ratio of the total energy loss rate of rotating quark to its linear drag part as a function of velocity for  $a/T \simeq 1.4$  (dashed), 12 (solid), 86 (dotted) curves.

Note that in this limit the velocity of string is close to  $v_c$  for all of the points. Using well-known relations between rotation and linear motion, constant velocity at each point of the rotating string and equation (B.8) one can see that the rate of energy loss is given by,

$$\frac{dE}{dt} = \frac{\Pi\omega}{2\pi\alpha'} = \frac{\mathcal{P}v}{2\pi\alpha'} = \frac{dE^{(\text{drag})}}{dt}. \quad (6.2)$$

This result is broken if the radius of the rotation for  $u_H > u \geq u_c$  ( $\rho(u) > \rho_c$ ) is larger than  $\rho_c$ , which means the constant velocity for all of the string's points is not good approximation. This is the case for small  $\omega$  but very large  $\Pi$ , discussed also in earlier sections.

It is easy to see that for larger  $\omega$  the dominant part of the rate of energy loss is due to the drag only for small velocities of the quark. As expected, in this limit the dominant part of the energy loss is due to the radiation for large enough velocities of the quark.

In [17], it was shown that for large  $\omega$  and large enough velocities of the quark, the dominant part of the energy loss is due to the radiation channel for isotropic  $\mathcal{N} = 4$  SYM plasma. This result was shown by comparing the energy loss with the synchrotron radiation introduced by Mikhailov [34]. So it is natural to compare the rate of energy loss with the synchrotron radiation using the Mikhailov's formula, which is the radiation of a quark rotating in a vacuum,

$$\left. \frac{dE}{dt} \right|_{\text{v. r.}} = \frac{\sqrt{\lambda}}{2\pi} \frac{v^2\omega^2}{(1-v^2)^2}. \quad (6.3)$$

Since this formula can describe the radiation in isotropic plasma [17], the ratio of the rate of energy loss (3.18) to the above rate (6.3) is actually the ratio of total energy loss to the radiation in isotropic plasma. The results are given in Fig. 10. For small  $\omega$  one can see that the total energy loss rate is much more than the radiation part, while in Fig. 9 we show that the dominant part of the energy loss, in this case, is due to the linear drag.

For large  $\omega$  and large enough velocity of the quark in Fig.10, where the dominant part of energy loss is due to the radiation, one can see that the radiation in anisotropic plasma is less than isotropic case and a larger  $a/T$ , causes to a smaller radiation. For fixed  $a/T$ , a larger velocity of the quark leads to a smaller ratio of the energy loss rate to the vacuum radiation such that for ultra-relativistic quarks with large  $\omega$ , the energy loss is closer to the vacuum radiation.

Again, one interesting range is intermediate angular velocity,  $\omega = 0.5$ , and large  $v$ . In this regime one can see the effect of anisotropy on the competition between the drag and

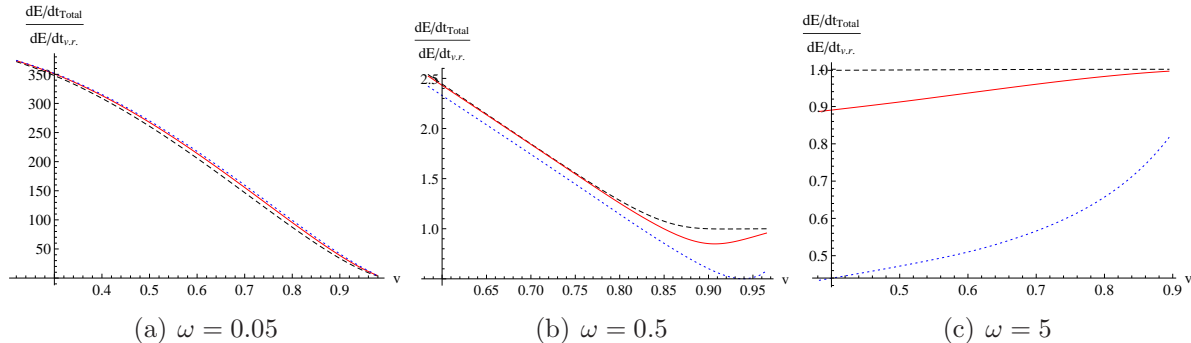


Figure 10: The ratio of the rate of energy loss to the radiation.  $a/T \simeq 0.8$ (dashed), 4.4(solid), 86(dotted) curves.

radiation channels in energy loss. This behavior is similar to the first row of Fig.7. Naively one can conclude that comparing the energy loss in the anisotropic and isotropic plasma at equal temperatures is more natural than at equal entropy densities.

## 7 Summary and discussion

In this paper, we have studied the energy loss of a rotating heavy quark in a strongly-coupled anisotropic plasma from holography. There are two models to investigate the anisotropic plasma from AdS/CFT correspondence which have been proposed by Mateos and Trancanelli in [20] and by Janik and Witaszczyk in [35].<sup>10</sup> In JW model [35], a geometry involving a comparatively benign naked singularity was considered, while MT model [20] has regular geometry involving a nontrivial axion field dual to a parity-odd deformation of the gauge theory. Different aspects of these models have been studied in [37]. The latter model has been used in this paper. In this model, the anisotropic  $\mathcal{N} = 4$  SYM plasma is symmetric in  $xy$  plane but in the beam direction ( $z$  direction) is not. Then in the context of heavy ion collisions, we considered a rotating test quark within the transverse plane which is also mostly interested in jets.

Holographic study shows different momentum broadening in an anisotropic medium along the beam axis and along the transverse plane [21, 22, 23]. These quantities in a weakly coupled anisotropic plasma have been studied in [38, 39, 40]. It was shown that, the momentum broadening along the beam axis increases slightly in the presence of anisotropy, while the momentum broadening in the transverse plane decreases more significantly. The jet quenching parameter was studied in [22, 23, 37] and it was found that for large anisotropic parameter the same result can be achieved. We showed that in the regime where we expect to see the radiation of beam of synchrotron-like radiation, the energy loss is significantly less than the isotropic case.

We find valuable results by comparing of the anisotropic case with the isotropic background at the same temperature or at the same entropy density. The ratio of the energy loss rate in anisotropic background to the isotropic case as a function of the velocity of the rotating quark is given in Fig. 7. One finds that the energy loss of ultra-relativistic heavy quark is the same as the drag force calculations in [21]. Also in Fig. 8, this ratio as a function of  $a/T$  for different velocities of rotating quark is shown. It is clearly seen that

<sup>10</sup>Other AdS backgrounds which are dual to an anisotropic fluids are constructed in [36]

the rate of energy loss in anisotropic background is smaller than the isotropic case and for fixed  $v$  and  $\omega$  the larger anisotropy leads to the smaller rate of energy loss.

It would be interesting to compare our results with the radiation energy loss of heavy quarks in a real anisotropic plasma. In a first-order opacity expansion it is studied in [33]. It was found that the energy loss due to the radiation depends on the direction of propagation of the fast partons with respect to the anisotropy axis as well as on the anisotropy parameter. It was shown that along parallel the anisotropy direction the radiation increases while in the transverse direction it decreases. Regarding our setup, we have considered the radiation in the transverse plane and we found that the radiation in a strongly-coupled anisotropic plasma is less than the isotropic case.

The energy density and angular distribution of the power radiated by a rotating quark in a strongly-coupled isotropic plasma was studied in [31]. This study was also extended to the case of non-zero temperature in [43]. It would be interesting to study effect of anisotropy on the angular distribution of the power radiated by a heavy quark rotating in an anisotropic plasma. We showed that the crossover from the drag-dominated regime to the radiation-dominated regime significantly depends on the anisotropic parameter. It was found that unlike in a vacuum, in the plasma at nonzero temperature the energy disturbance created by the rotating quark can excite in two qualitatively distinct modes in the energy density; a sound mode and a light-like mode which propagates at the speed of light. The energy loss due to unstable modes in a weakly coupled anisotropic plasma has been studied in [41, 42]. It would be very interesting to understand the effect of instability modes on the energy density in an anisotropic strongly-coupled plasma. This investigation can shed new light to the similarities between the quenching of the beam of strongly-coupled synchrotron radiation in the strongly-coupled anisotropic  $\mathcal{N} = 4$  SYM plasma and the quenching of jets in heavy ion collisions at the LHC and RHIC.

### Acknowledgements

We would like to thank M. Ali-Akbari, N. Abbasi, A. Davody, M. Abedini, E. Azimfard, D. Giataganas, K. Goldstein D. Nickel and M. M. Sheikh-Jabbari for useful discussions on the different aspects of rotating string in an anisotropic background. We are also very grateful to thank to K. Goldstein and M. Sohani for carefully reading the draft. K. B. F. thanks a lot from M. Strickland for discussion on the papers in the subject of weakly anisotropic plasma. H. S. thanks R. Warmbier and R. Morad for their comments on numerical calculations. We would like to thank the referee of JHEP for giving constructive comments which helped improving the paper. H. S. would like to thank Institute for Research in Fundamental Sciences (IPM) for hospitality during different stages of preparing this project. H. S. is supported by National Research Foundation (NRF). Any opinion, findings and conclusions or recommendations expressed in this material are those of the H. S. and therefore the NRF do not accept any liability with regard thereto.

## A Rotation in anisotropic plane

In this appendix we study a rotating quark in a general three dimensional spatial of an anisotropic background (2.1). Without loss of generality, we assume that the rotation is in  $xz$ -plane (extension to more general case is straightforward). Using the following polar

coordinate transformation

$$x = \rho \cos \psi, \quad z = \frac{\rho}{\sqrt{H}} \sin \psi, \quad (\text{A.1})$$

which is useful to study a rotating object, one can show that the  $xz$  part of the background metric (2.1) is given by

$$dx^2 + H dz^2 = d\rho^2 + \rho^2 d\psi^2 + \frac{\rho^2 \sin^2 \psi}{4} \frac{H'^2}{H^2} du^2 + \rho \sin^2 \psi \frac{H'}{H} dud\rho - \frac{\rho^2 \sin 2\psi}{2} \frac{H'}{H} dud\psi. \quad (\text{A.2})$$

It's obvious that there is no SO(2) symmetry in  $xz$ -plane for  $\mathcal{H} \neq \text{constant}$ . As we will see this has important consequence to find the energy loss rate.

Using the usual ansatz for a rotating string in  $xz$ -plane,

$$X^\mu(\tau, \sigma) = (t = \tau, u = \sigma, \psi = \omega t + \theta(\sigma), \rho = \rho(u), y = 0), \quad (\text{A.3})$$

it is easy to show that the Lagrangian density of Nambu-Goto action for a rotating string in  $xz$ -plane is given by

$$\mathcal{L} = \left[ -(G_{uu} + G_{\rho\rho}\rho'^2 + 2G_{u\rho}\rho')(G_{tt} + G_{\psi\psi}\omega^2) - G_{tt}G_{\psi\psi}\theta'^2 - G_{u\psi}(2G_{tt}\theta' - G_{u\psi}\omega^2) \right]^{1/2} \quad (\text{A.4})$$

Note that the  $G_{uu}$ ,  $G_{u\rho}$  and  $G_{u\psi}$  components of the background are functions of both  $u$  and  $\psi$  coordinates. Again, it shows that there is no SO(2) symmetry in this case. In contrast to the rotation in  $xy$ -plane, studied in the main body of the paper, not only  $\theta'$  (the derivative of  $\theta$  with respect to  $u$ ), but also  $\theta$  appears explicitly in the action (via  $\psi$  dependency),

$$\mathcal{L} = \mathcal{L}(\rho, \rho', \theta, \theta'). \quad (\text{A.5})$$

It means the momentum conjugate to the  $\theta$  field is not a constant of motion anymore and a hanging string rotates in-homogeneously.

On the other hand, from drag force investigations [21] we know that for a string moving in  $xz$ -plane along neither  $x$  nor along  $z$  directions, there is a misalignment between the velocity in the far infrared and the drag force  $\vec{F}$ . This is the main reason for disability of usual (holographic) calculation of a rotating quark in an anisotropic plane which leads to the inhomogeneous rotation explained above. It's interesting to solve the equations of motion of  $\rho$  and  $\theta$  fields (two coupled second order differential equations) in anisotropic background for a general rotation in anisotropic background which is not in the scope of this paper.

## B Linear drag in a general background

In this appendix we give a brief review on a linear drag case corresponded to a quark moving on a line with a fixed velocity  $v$  in a general background which has been known for some especial examples [12]. Using the static gauge for a string moving in  $x$  direction of a general background (3.1)

$$X_{\text{drag}}^\mu(\tau, \sigma) = (t = \tau, u = \sigma, x = \xi(u) + vt, y = z = 0), \quad (\text{B.1})$$

one can show that the Nambu-Goto density of lagrangian is given by

$$\mathcal{L}_{\text{drag}} = [-G_{tt}G_{uu} - G_{xx}G_{tt}\xi'^2 - G_{xx}G_{uu}v^2]^{1/2}. \quad (\text{B.2})$$

Since  $\xi$  does not appear explicitly in the action, its momentum conjugate is conserved and the equation of motion is given by

$$\mathcal{P} = \frac{\partial \mathcal{L}}{\partial \xi'} = -\frac{G_{tt}G_{xx}\xi'}{\mathcal{L}} = \text{constant}. \quad (\text{B.3})$$

Solving this equation for  $\xi'$  yields to

$$\xi'^2 = -\mathcal{P}^2 \frac{G_{uu}(G_{tt} + G_{xx}v^2)}{G_{xx}G_{tt}(G_{xx}G_{tt} + \mathcal{P}^2)}. \quad (\text{B.4})$$

The positivity of LHS leads to the fact that there is a critical point,  $u_c^{(\text{drag})}$ , where both numerator and denominator change their signs and it is defined by

$$G_{tt}(u_c)^{(\text{drag})} + G_{xx}(u_c)^{(\text{drag})}v^2 = 0, \quad (\text{B.5})$$

$$G_{xx}(u_c)^{(\text{drag})}G_{tt}(u_c)^{(\text{drag})} + \mathcal{P}^2 = 0, \quad (\text{B.6})$$

which lead to

$$|G_{tt}(u_c)^{(\text{drag})}| = \mathcal{P}v, \quad G_{xx}(u_c)^{(\text{drag})} = \frac{\mathcal{P}}{v}. \quad (\text{B.7})$$

On the other hand, by using (B.5) and (B.6), it is easy to show that the rate of energy loss due to the linear drag is given by

$$\frac{dE^{(\text{drag})}}{dt} = \Pi_t^{\sigma(\text{drag})} = \frac{\mathcal{P}v}{2\pi\alpha'} = \frac{|G_{tt}(u_c)^{(\text{drag})}|}{2\pi\alpha'}, \quad (\text{B.8})$$

where in the second equality we used the first equation in (B.7). Comparing equations (3.18) and (B.8) shows that the general form of the rate of energy loss in both linear drag and rotating strings are the same and it's just a function of the critical point.

Therefore, if the critical point at two different cases are the same the rate of energy loss should be the same. As we show in sections 4 and 5, for small angular velocity of a rotating string the critical point is very close to the linear drag both numerically and analytically.

## References

- [1] J. Casalderrey-Solana, H. Liu, D. Mateos, K. Rajagopal and U. A. Wiedemann, "Gauge/String Duality, Hot QCD and Heavy Ion Collisions," arXiv:1101.0618 [hep-th].
- [2] The ALICE Collaboration, K. Aamodt et al., "Elliptic flow of charged particles in Pb-Pb collisions at 2.76 TeV," arXiv:1011.3914 [nucl-ex].
- [3] P. Romatschke and M. Strickland, "Collective modes of an anisotropic quark gluon plasma," Phys. Rev. D **68** (2003) 036004 [hep-ph/0304092].

- [4] P. B. Arnold, G. D. Moore and L. G. Yaffe, “The Fate of non-Abelian plasma instabilities in 3+1 dimensions,” *Phys. Rev. D* **72** (2005) 054003 [hep-ph/0505212].
- [5] A. Rebhan, M. Strickland and M. Attems, “Instabilities of an anisotropically expanding non-Abelian plasma: 1D+3V discretized hard-loop simulations,” *Phys. Rev. D* **78** (2008) 045023 [arXiv:0802.1714 [hep-ph]].
- [6] J. M. Maldacena, “The large N limit of superconformal field theories and supergravity,” *Adv. Theor. Math. Phys.* **2** (1998) 231 [*Int. J. Theor. Phys.* **38** (1999) 1113] [arXiv:hep-th/9711200].
- [7] S. S. Gubser, I. R. Klebanov and A. M. Polyakov, “Gauge theory correlators from non-critical string theory,” *Phys. Lett. B* **428** (1998) 105 [arXiv:hep-th/9802109].
- [8] E. Witten, “Anti-de Sitter space and holography,” *Adv. Theor. Math. Phys.* **2** (1998) 253 [arXiv:hep-th/9802150].
- [9] E. Witten, “Anti-de Sitter space, thermal phase transition, and confinement in gauge theories,” *Adv. Theor. Math. Phys.* **2** (1998) 505 [arXiv:hep-th/9803131].
- [10] H. Liu, K. Rajagopal and U. A. Wiedemann, “Calculating the jet quenching parameter from AdS/CFT,” *Phys. Rev. Lett.* **97** (2006) 182301 [hep-ph/0605178].
- [11] C. P. Herzog, A. Karch, P. Kovtun, C. Kozcaz and L. G. Yaffe, “Energy loss of a heavy quark moving through N=4 supersymmetric Yang-Mills plasma,” *JHEP* **0607** (2006) 013 [arXiv:hep-th/0605158].
- [12] S. S. Gubser, “Drag force in AdS/CFT,” *Phys. Rev. D* **74** (2006) 126005 [arXiv:hep-th/0605182].
- [13] S. S. Gubser, S. S. Pufu, F. D. Rocha and A. Yarom, “Energy loss in a strongly coupled thermal medium and the gauge-string duality,” arXiv:0902.4041 [hep-th];  
M. Chernicoff, J. A. Garcia, A. Guijosa and J. F. Pedraza, “Holographic Lessons for Quark Dynamics,” *J. Phys. G G* **39** (2012) 054002 [arXiv:1111.0872 [hep-th]];  
N. Abbasi and A. Davody, “Moving Quark in a Viscous Fluid,” arXiv:1202.2737 [hep-th];  
K. B. Fadafan, “Charge effect and finite 't Hooft coupling correction on drag force and Jet Quenching Parameter,” *Eur. Phys. J. C* **68** (2010) 505 [arXiv:0809.1336 [hep-th]];  
K. B. Fadafan, “R\*\*2 curvature-squared corrections on drag force,” *JHEP* **0812** (2008) 051 [arXiv:0803.2777 [hep-th]];  
J. Sadeghi and B. Pourhassan, “STU/QCD Correspondence,” arXiv:1205.4254 [hep-th].
- [14] F. Dominguez, C. Marquet, A. H. Mueller, B. Wu and B. -W. Xiao, “Comparing energy loss and p-perpendicular - broadening in perturbative QCD with strong coupling N = 4 SYM theory,” *Nucl. Phys. A* **811** (2008) 197 [arXiv:0803.3234 [nucl-th]].
- [15] M. Chernicoff and A. Guijosa, “Acceleration, Energy Loss and Screening in Strongly-Coupled Gauge Theories,” *JHEP* **0806** (2008) 005 [arXiv:0803.3070 [hep-th]].

- [16] Y. Hatta, E. Iancu, A. H. Mueller and D. N. Triantafyllopoulos, “Radiation by a heavy quark in N=4 SYM at strong coupling,” Nucl. Phys. B **850** (2011) 31 [arXiv:1102.0232 [hep-th]].
- [17] K. B. Fadafan, H. Liu, K. Rajagopal and U. A. Wiedemann, “Stirring Strongly Coupled Plasma,” Eur. Phys. J. C **61** (2009) 553 [arXiv:0809.2869 [hep-ph]].
- [18] M. Ali-Akbari and U. Gursoy, “Rotating strings and energy loss in non-conformal holography,” JHEP **1201** (2012) 105 [arXiv:1110.5881 [hep-th]].
- [19] E. Kiritsis and G. Pavlopoulos, “Heavy quarks in a magnetic field,” JHEP **1204** (2012) 096 [arXiv:1111.0314 [hep-th]].
- [20] D. Mateos and D. Trancanelli, “The anisotropic N=4 super Yang-Mills plasma and its instabilities,” Phys. Rev. Lett. **107** (2011) 101601 [arXiv:1105.3472 [hep-th]];  
D. Mateos and D. Trancanelli, “Thermodynamics and Instabilities of a Strongly Coupled Anisotropic Plasma,” JHEP **1107** (2011) 054 [arXiv:1106.1637 [hep-th]].
- [21] M. Chernicoff, D. Fernandez, D. Mateos and D. Trancanelli, “Drag force in a strongly coupled anisotropic plasma,” arXiv:1202.3696 [hep-th].
- [22] D. Giataganas, “Probing strongly coupled anisotropic plasma,” arXiv:1202.4436 [hep-th].
- [23] M. Chernicoff, D. Fernandez, D. Mateos and D. Trancanelli, “Jet quenching in a strongly coupled anisotropic plasma,” arXiv:1203.0561 [hep-th].
- [24] A. Guijosa and J. F. Pedraza, “Early-Time Energy Loss in a Strongly-Coupled SYM Plasma,” JHEP **1105** (2011) 108 [arXiv:1102.4893 [hep-th]].
- [25] P. Kovtun, D. T. Son and A. O. Starinets, “Viscosity in strongly interacting quantum field theories from black hole physics,” Phys. Rev. Lett. **94** (2005) 111601 [hep-th/0405231].
- [26] A. Rebhan and D. Steineder, “Violation of the Holographic Viscosity Bound in a Strongly Coupled Anisotropic Plasma,” Phys. Rev. Lett. **108** (2012) 021601 [arXiv:1110.6825 [hep-th]].
- [27] K. A. Mamo, “Holographic Wilsonian RG Flow of the Shear Viscosity to Entropy Ratio in Strongly Coupled Anisotropic Plasma,” arXiv:1205.1797 [hep-th].
- [28] M. Brigante, H. Liu, R. C. Myers, S. Shenker and S. Yaida, “The Viscosity Bound and Causality Violation,” Phys. Rev. Lett. **100** (2008) 191601 [arXiv:0802.3318 [hep-th]];  
Y. Kats and P. Petrov, “Effect of curvature squared corrections in AdS on the viscosity of the dual gauge theory,” JHEP **0901** (2009) 044 [arXiv:0712.0743 [hep-th]].
- [29] T. Azeyanagi, W. Li and T. Takayanagi, “On String Theory Duals of Lifshitz-like Fixed Points,” JHEP **0906** (2009) 084 [arXiv:0905.0688 [hep-th]].
- [30] K. B. Fadafan, “Drag force in asymptotically Lifshitz spacetimes,” arXiv:0912.4873 [hep-th].

- [31] C. Athanasiou, P. M. Chesler, H. Liu, D. Nickel and K. Rajagopal, “Synchrotron radiation in strongly coupled conformal field theories,” *Phys. Rev. D* **81** (2010) 126001 [Erratum-ibid. *D* **84** (2011) 069901] [arXiv:1001.3880 [hep-th]].
- [32] P. M. Chesler, K. Jensen, A. Karch and L. G. Yaffe, “Light quark energy loss in strongly-coupled  $N = 4$  supersymmetric Yang-Mills plasma,” *Phys. Rev. D* **79** (2009) 125015 [arXiv:0810.1985 [hep-th]].
- [33] P. Roy and A. K. Dutt-Mazumder, “Radiative energy loss in an anisotropic Quark-Gluon-Plasma,” *Phys. Rev. C* **83** (2011) 044904 [arXiv:1009.2304 [nucl-th]].
- [34] A. Mikhailov, “Nonlinear waves in AdS / CFT correspondence,” hep-th/0305196.
- [35] R. A. Janik and P. Witaszczyk, “Towards the description of anisotropic plasma at strong coupling,” *JHEP* **0809** (2008) 026 [arXiv:0806.2141 [hep-th]].
- [36] J. Erdmenger, P. Kerner and H. Zeller, “Transport in Anisotropic Superfluids: A Holographic Description,” *JHEP* **1201** (2012) 059 [arXiv:1110.0007 [hep-th]]. I. Gahramanov, T. Kalaydzhyan and I. Kirsch, “Anisotropic hydrodynamics, holography and the chiral magnetic effect,” arXiv:1203.4259 [hep-th].
- [37] A. Rebhan and D. Steineder, “Probing Two Holographic Models of Strongly Coupled Anisotropic Plasma,” arXiv:1205.4684 [hep-th].
- [38] P. Romatschke and M. Strickland, “Collisional energy loss of a heavy quark in an anisotropic quark-gluon plasma,” *Phys. Rev. D* **71** (2005) 125008 [hep-ph/0408275].
- [39] P. Romatschke, “Momentum broadening in an anisotropic plasma,” *Phys. Rev. C* **75** (2007) 014901 [hep-ph/0607327].
- [40] A. Dumitru, Y. Nara, B. Schenke and M. Strickland, “Jet broadening in unstable non-Abelian plasmas,” *Phys. Rev. C* **78** (2008) 024909 [arXiv:0710.1223 [hep-ph]].
- [41] M. E. Carrington, K. Deja and S. Mrowczynski, “Parton Energy Loss in an Unstable Quark-Gluon Plasma,” arXiv:1110.4846 [hep-ph].
- [42] A. Kurkela and G. D. Moore, “Thermalization in Weakly Coupled Nonabelian Plasmas,” *JHEP* **1112** (2011) 044 [arXiv:1107.5050 [hep-ph]].
- [43] P. M. Chesler, Y. -Y. Ho and K. Rajagopal, “Shining a Gluon Beam Through Quark-Gluon Plasma,” arXiv:1111.1691 [hep-th].